BIOCHEMISTRY
including biophysical chemistry & molecular biology
Article

Biochemistry **2010,** *49,* 3593–3601 3593
DOI: 10.1021/bi1003537

Supermetalation of the β Domain of Human Metallothionein 1a[†]

Duncan E. K. Sutherland, Mathew J. Willans, and Martin J. Stillman*

Department of Chemistry, The University of Western Ontario, London, ON, Canada N6A 5B7

Received March 8, 2010; Revised Manuscript Received March 22, 2010

ABSTRACT: Metallothionein has been implicated in a number of functions, including toxic metal detoxification, as a metal chaperone and in metal ion homeostasis. In this paper, we demonstrate that the β domain of human metallothionein 1a, well-known to bind three Zn^{2+} or Cd^{2+} ions with nine cysteinyl sulfurs, is also capable of binding an additional Cd^{2+} ion, leading to the formation of the supermetalated Cd_4-β-rhMT 1a. This intermediate, either by itself or in concert with the α domain of human metallothionein, is a likely model for metal exchange with the apoenzyme, which is one of the key roles of metallothionein. Through electrospray ionization (ESI) mass spectrometry and circular dichroism (CD) and ultraviolet (UV) spectroscopy, we show that the addition of 4.4 molar equiv of $CdSO_4$ to a solution of Cd_3-β-rhMT 1a leads to the complete conversion to Cd_4-β-rhMT 1a. ESI mass spectrometry was used to determine the exact speciation of β-rhMT 1a. While the UV absorption spectrum increased slightly, the CD spectrum of Cd_4-β-rhMT 1a showed significant changes with the appearance of a sharp monophasic peak at 252 nm in contrast to the derivative-shaped envelope of the Cd_3-β-rhMT 1a species [peak extrema at (+)262 and (−)236 nm], indicating disruption of the exciton coupling in the metal−thiolate cluster. Additionally, both direct and indirect ^{113}Cd nuclear magnetic resonance (NMR) spectra of the Cd_3-β-rhMT 1a and Cd_4-β-rhMT 1a species were recorded. The ^{113}Cd NMR spectrum of Cd_4-β-rhMT 1a contained four cadmium peaks in the tetrahedral thiolate region at 688.8, 650.3, 635.9, and 602.5 ppm. This represents the first report of both NMR data for isolated Cd_3-β-rhMT 1a and supermetalated Cd_4-β-rhMT 1a.

Metallothionein (MT),[1] first characterized in 1957 (*1*), is a cysteine-rich protein implicated in heavy metal detoxification, metal ion homeostasis, and protection against oxidative stress (*2*, *3*). However, despite half a century of intensive research, specific roles for MT in living organisms are still largely unknown. One of the reasons for the uncertainty is the fact that until very recently the mechanism of metalation of metallothionein was thought to proceed in a cooperative manner (*4*, *5*), in which the binding of one metal acts to facilitate the binding of subsequent metals. In this model, the only structures of biological significance would be the fully metalated or completely demetalated species, and any partially metalated species would likely be too unstable to have a specific role. However, new studies have shown the mechanism of metalation to be in fact noncooperative for Cd^{2+} and Zn^{2+} (*6*−*8*), as well as As^{3+} (*9*, *10*); significantly, a noncooperative mechanism allows for partially metalated and metal-exchange intermediates to be stable and, therefore, to be able to take part in cellular chemistry.

To further complicate matters, recent papers have proposed the existence of supermetalated forms of metallothionein, that is proteins where the level of metalation is in excess of normal maximum levels, calling into question the so-called "magic numbers" of metal binding (*11*). Supermetalated forms have been reported for a single additional cadmium ion binding to both the isolated α domain of human MT-1a (Cd_5-α-rhMT 1a) (*12*) and human MT-3 (Cd_8-βα-hMT 3) (*13*). Because the cadmium ions in MT-1 and -2 isomorphously replace zinc ions, these results suggest that this additional metal site may be involved with metal ion homeostasis and may be considered as a model for metal-exchange intermediates. In addition, the supermetalated site may also be connected with the mechanism for binding of incoming metals with binding affinities greater than that for the resident zinc, for example, the essential copper(I) and the toxic cadmium(II). To account for the supermetalation of hMT-3, Meloni et al. (*13*) proposed the involvement of both the α and β domains in the stabilization of the additional metal ion. However, previous studies involving the oxidation of hMT-3 with nitric oxide (*14*), as well as the lack of long-range interdomain NOEs in the solution structure of hMT-3 (*15*), in fact suggest that little domain interaction is involved. Taken together, these metalation properties emphasize the need for precise information about the specific properties of the individual domains in defining the function of MT as a whole.

The many members of the metallothionein family have each developed unique metal binding sites and domain structures, with different metal binding properties. Mammalian metallothionein consists of a total of 20 cysteine residues (nine in the N-terminal β domain capable of binding three Zn^{2+} or Cd^{2+} ions and 11 in the C-terminal α domain capable of binding four Zn^{2+} or Cd^{2+} ions) (*16*). The seaweed *Fucus vesiculosus* form contains a total of 16 cysteine residues (seven in an as yet uncharacterized N-terminal γ domain and nine in the C-terminal β domain, both able to bind three Zn^{2+} or Cd^{2+} ions) (*17*). Each of these proteins

[†]We thank NSERC of Canada for financial support through operating funds (to M.J.S.) and an Alexander Graham Bell Canada Graduate Scholarship (CGS) (to D.E.K.S.).

*To whom correspondence should be addressed. Telephone: (519) 661-3821. Fax: (519) 661-3022. E-mail: martin.stillman@uwo.ca.

[1]Abbreviations: MT, metallothionein; β-rhMT 1a, recombinantly prepared β domain of human metallothionein isoform 1a; α-rhMT 1a, recombinantly prepared α domain of human metallothionein isoform 1a; βα-rhMT 1a, recombinantly prepared human metallothionein isoform 1a; HSQC, heteronuclear single-quantum coherence; ESI, electrospray ionization; MS, mass spectrometry; CD, circular dichroism; NMR, nuclear magnetic resonance.

Published on Web 03/23/2010

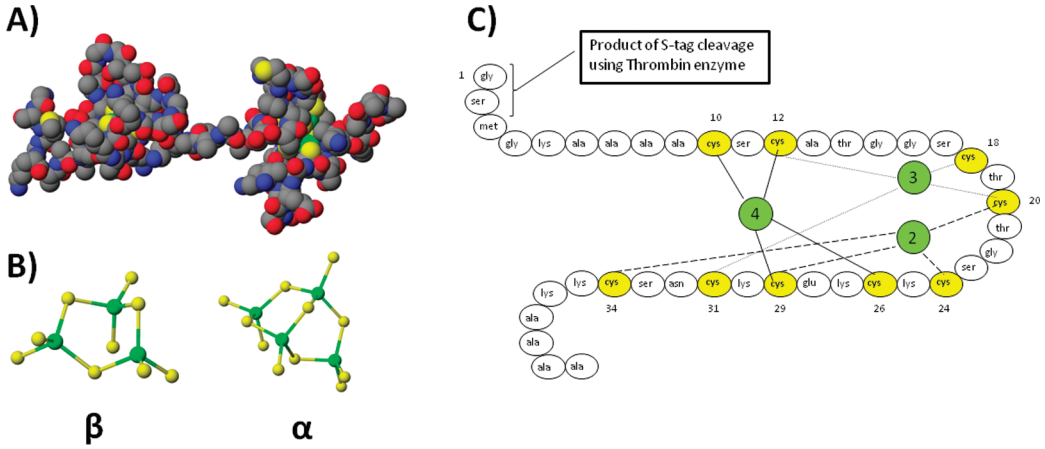

FIGURE 1: (A) Space filling structure of Cd_7-$\beta\alpha$-rhMT 1a calculated using molecular modeling. The N-terminal β domain is located on the left-hand side, while the C-terminal α domain is located on the right-hand side. (B) The cadmium−cysteinyl−thiolate clusters of Cd_7-$\beta\alpha$-rhMT 1a are presented as a ball-and-stick model: β domain (left) and α domain (right). (C) Connectivity diagram of the β domain of human metallothionein 1a, which shows that each of the three traditional cadmium atoms is connected to exactly four cysteine amino acids. The connectivity diagram has been renumbered to allow for both the amino acids glycine and serine, a product of S-tag cleavage with thrombin, located on the N-terminus of the domain. The numbering of the cadmium−thiolate centers is based on the NMR assignment by Messerle et al. (*27*). Molecular modeling data from Chan et al. (*28*).

uses the thiolate sulfur of cysteine residues to coordinate the bound metals. Other coordinating amino acids have also been identified, with bacterial metallothionein SmtA binding four Zn^{2+} atoms through nine cysteine and two histidine residues (*18*). Furthermore, the Zn^{2+} atom coordinated to the two histidine residues was inert to metal exchange, and it was postulated that this stable metal allowed the maintenance of the structure during metal depletion. Recently, the C-terminal β_E domain of *Tricium aestivum*, a common wheat consisting of two metal−thiolate domains with 17 cysteine residues (six in the N-terminal domain capable of binding two Zn^{2+} or Cd^{2+} ions and 11 in the β_E domain capable of binding four Zn^{2+} or Cd^{2+} ions), was found to have both a traditional β-like domain and a fourth zinc coordinated to two cysteine and two histidine residues in close proximity (*19*). Of significant interest is human metallothionein 3 (hMT-3), with approximately 70% sequence homology with hMT-2; hMT-3 is expressed predominantly in the central nervous system and inhibits neuronal growth (*20*). The addition of a single threonine (Thr5) in a TCPCP motif (*21*) and a glutamate-rich hexapeptide (*22*) near the C-terminus have been shown to be critical to the function and labilization of Zn^{2+} atoms, respectively. Interestingly, Romero-Isart et al. were able to engineer neuronal activity of hMT-3 into hMT-1 by addition of the TCPCP inset, which suggests the two isoforms may differ in only the slight cluster arrangements caused by three distinct mutations (*21*). Analysis of the isolated domains demonstrated that the ability to inhibit neuronal growth resides in the β domain alone, and that this ability results from its unique sequence, suggesting preferential interaction with target proteins (*23*). These β domain-centered protein−protein interactions have not been well characterized because of a general lack of information available about this domain for all metallothionein isoforms.

Human metallothionein 1a (Figure 1A) consists of two independent domains each encapsulating a metal−thiolate core (Figure 1B). The sequence of the cleaved recombinant β domain of human metallothionein 1a (β-rhMT 1a), shown in Figure 1C, with cadmium atoms colored green and cysteine residues yellow, contains both a glycine and serine residue from the thrombin cleavage reaction. This fragment encompasses residues from Cys5 to Lys31 of human metallothionein 1a. The numbering of the cadmium−thiolate core is cross referenced to the original naming conventions based on the order of the NMR bands in the mammalian MT-2a spectra (*24*), while the numbering of the cysteine residues has been adjusted to accommodate both the additional amino acids from thrombin cleavage (residues 1 and 2) and a series of amino acids meant to aid in protein expression (residues 3−9). The β-MT polypeptide backbone wrapping of the metal−thiolate core proceeds in a right-handed manner, as opposed to the left-handed wrapping of α-MT. While properties of the α metal binding site, Cd_4-α-rhMT, have been well documented through structural studies of both the isolated domain (*12*, *25*) and the domain as part of the whole protein (*16*), far less structural information has been reported for the isolated β metal binding site, Cd_3-β-rhMT. Analysis of the NMR data for β-rhMT in human metallothionein suggested that fluxionality causes a decrease in the intensity of the one-dimensional (1D) ^{113}Cd signals. Further compounding this problem is the inability of metallothionein to readily crystallize. To date, only two crystal structures have been reported, including rat Cd_5Zn_2-MT-2 and much later a Cu_8-yeast metallothionein (*16*, *26*). To determine such basic in vivo data as protein binding partners and metalation status, the complete metalation properties of β-MT must be fully characterized, particularly when one considers the β-centered reactions in hMT-3.

The metal transfer function in MT has been well documented, with Zn(II) transfer taking place from the fully metalated Zn_7-$\beta\alpha$-MT to *m*-aconitase (*29*), carbonic anhydrase (*30*), and the prototypical transcription factor, Gal4 (*31*). These studies have shown the importance of protein−protein interactions. However, no zinc-exchange intermediate that provides insight into the actual mechanism of metal transfer has been characterized.

In this study, we present evidence that the isolated β domain of human metallothionein 1a, Cd_3-β-rhMT 1a, is capable of binding an additional cadmium atom, forming Cd_4-β-rhMT 1a. Exact metal speciation was monitored using ESI mass spectrometry (ESI-MS), which allowed for a direct correlation between the number of cadmium atoms bound to the protein and changes observed via UV and CD spectroscopy. To ensure that the metal was interacting directly with the metal−thiolate cluster, both direct and indirect ^{113}Cd NMR spectroscopy were used. Addition of excess Cd^{2+}, in

the form of solid $^{113}CdCl_2$, produced four cadmium signals in the range of 600−700 ppm, which corresponds to the chemical shift region expected for cadmium bound to the thiolates. When considering these results in the context of the supermetalated Cd_5-α-rhMT 1a (*12*) and Cd_8-βα-hMT 3 (*13*), two possible scenarios arise. (1) Both domains, when present, work in concert to accept an additional cadmium atom, or (2) both domains are individually capable of supermetalation. In either case, supermetalation must be fully characterized to understand its chemical implications that will have consequences at a cellular level.

EXPERIMENTAL PROCEDURES

Chemicals. The following chemicals were used: cadmium sulfate (Fisher Scientific), cadmium(113) chloride (Trace Sciences International Inc.), deuterium oxide (Cambridge Isotopes Laboratories, Inc.), tris(2-carboxyethyl)phosphine (Pierce), Thrombin-CleanCleave Kit (Sigma) Tris buffer and tris(hydroxymethyl)-aminomethane (EMD Chemicals/VWR), ammonium formate buffer (J. T. Baker), ammonium hydroxide (Caledon Laboratory Chemicals), formic acid (Caledon Laboratory Chemicals), and hydrochloric acid (Caledon Laboratory Chemicals). All solutions were made with >16 MΩ cm deionized water (Barnstead Nanopure Infinity). HiTrap SP HP ion-exchange columns (Amersham Biosciences/GE Healthcare), superfine G-25 Sephadex (Amersham Biosciences/GE Healthcare), and stirred ultrafiltration cell models 8010 and 8200 (Amicon Bioseparations/Millipore) with a YM-3 membrane (3000 molecular weight cutoff) were used in the protein purification steps.

Protein Preparation. The expression and purification methods have been previously reported (*28*). The β-rhMT 1a used in this study was based on the 38-residue sequence MGKAAAA-CSC ATGGSCTCTG SCKCKECKCN SCKKAAAA with no disulfide bonds present in the system. The expression system included, for the purpose of stability, an N-terminal S-tag (MKETAAAKFE RQHMDSPDLG TLVPRGS). Recombinant β-rhMT 1a was expressed in *Escherichia coli* BL21(DE3) transformed using the pET29a plasmid. Removal of the S-tag was performed using a Thrombin CleanCleave Kit. To impede oxidation of the cysteine residues to disulfide bonds, all protein samples were saturated with argon and rigorously evacuated.

CD and UV Spectroscopic and ESI-MS Measurements. A solution of Cd_3-β-rhMT 1a was prepared in 5 mM ammonium formate (pH 9.0) to a concentration of 24.4 μM for CD and UV spectroscopic and ESI-MS studies, and all measurements were performed on the same sample for a given excess of molar equivalents. The protein concentrations was confirmed by UV absorption spectroscopy using the absorbance at 250 nm, which corresponds to the ligand-to-metal charge transfer transition generated by the metal−thiolate bond (ε_{250} = 36000 M^{-1} cm^{-1}). Cadmium sulfate was prepared in H_2O, to a final concentration of 11.4 mM. Both the cadmium sulfate concentration and all molar equivalents were determined through calibration of the Cd^{2+} content in solution using atomic absorption spectroscopy (AAS).

Spectra were recorded for the Cd_3-β-rhMT 1a solution (24.4 μM) in 5 mM ammonium formate buffer (pH 9.0) and for the same solution of Cd_3-β-rhMT 1a to which 4.4 excess molar equivalents of Cd^{2+} had been added, forming (as we show in the ESI-MS data) Cd_4-β-rhMT 1a. CD spectra were recorded on a Jasco J810 spectropolarimeter in a 1 cm quartz cuvette at room temperature (22 °C) using Spectra Manager version 1.52.01 (Jasco). The wavelength range of 200−350 nm was scanned continuously at a rate of 60 nm/min with a bandwidth of 2 nm. The spectral data were organized and plotted using Origin version 7.0383. The CD spectra are expressed in units of Δ*A*. UV spectra were recorded on a Cary 5G UV−vis−NIR spectrophotometer (Varian Canada, Mississauga, ON) in a 1 cm quartz cuvette at room temperature (22 °C) using the Cary Win UV Scan software application. The wavelength range of 200−350 nm was scanned continuously. All spectra were baseline-corrected. The spectral data were organized and plotted using Origin version 7.0383.

ESI-MS measurements were taken after the UV absorption and CD spectroscopic experiments had been completed. Mass spectra were recorded on a Micromass LCT electrospray ionization time-of-flight (ESI-TOF) mass spectrometer (Waters Micromass) at room temperature (22 °C) using Mass Lynx version 4.0. The ESI-TOF instrument was calibrated with a solution of NaI. The scan conditions for the spectrometer were as follows: capillary, 3000.0 V; sample cone, 15.0 V; extraction cone, 10.0 V; RF lens, 450.0 V; desolvation temperature, 20.0 °C; source temperature, 80.0 °C; nebulizer gas flow, 53 L/h; and desolvation gas flow, 548 L/h. The *m*/*z* range was 500.0−3000.0; the scan mode was continuum, and the interscan delay was 0.10 s. Max Ent 1 from the Mass Lynx version 4.0 (Waters Micromass, Mississauga, ON) was used for the spectral reconstruction program.

NMR Spectroscopic Measurements. We prepared β-rhMT 1a NMR samples by pooling the protein product from five 4 L recombinant preparations following thrombin cleavage of the S-tag. The $^{113}Cd_3$-β-rhMT 1a used for acquisition of all NMR spectra was prepared by addition of concentrated formic acid to demetallate the protein, followed by desalting on a G-25 Sephadex column at which point tris(2-carboxyethyl)phosphine (TCEP) was added to the solution to impede oxidation. Cadmium(113) chloride was added to the solution followed by neutralization using ammonium hydroxide. The solution was then concentrated to 10 mL and desalted into 10 mM ammonium formate buffer using a G-25 Sephadex column at pH 7.5 to remove any excess cadmium(113). Concentration and D_2O exchange were performed using stirred ultrafiltration cell models 8200 and 8010, respectively. The final protein concentration was determined to be 7−8 mM based on UV absorption spectroscopy using the 250 nm peak (ε_{250} = 36000 M^{-1} cm^{-1}). The buffer used to determine the sample concentration in the NMR tube was 10 mM Tris-HCl (pH 7.4). The sample was saturated with argon and sealed in a 5 mm NMR tube for analysis. Following acquisition of $^{113}Cd_3$-β-rhMT and $^{113}Cd_4$-β-rhMT, excess cadmium(113) was added to produce $^{113}Cd_4$-β-rhMT 1a used for both the 1D and two-dimensional (2D) NMR spectra.

All NMR spectra were acquired on a Varian Inova 600 NMR spectrometer [$\nu_L(^1H)$ = 599.44 MHz, and $\nu_L(^{113}Cd)$ = 132.99 MHz] using Varian's VNMRJ 2.2D with the Chempack 3.0 add-on. The ^{113}Cd chemical shifts were referenced with respect to an external 1.0 M solution of $CdSO_4$ in D_2O [$\delta(^{113}Cd)$ = 0.0 ppm], while ^1H chemical shifts were internally referenced to TMS [$\delta(^1H)$ = 0.0 ppm] on the basis of the ^2H frequency of the deuterated solvent.

Direct-detect 1D $^{113}Cd\{^1H\}$ NMR spectra were recorded using a Varian broad-band 5.0 mm HX probe, a spectral range from 540 to 740 ppm, and WALTZ-16 ^1H decoupling during acquisition only. For the mixture of Cd_3-β-rhMT 1a and Cd_4-β-rhMT 1a, a total of 93000 transients accumulated using a relaxation delay of 1 s and a 90° pulse width of 16.2 μs with an

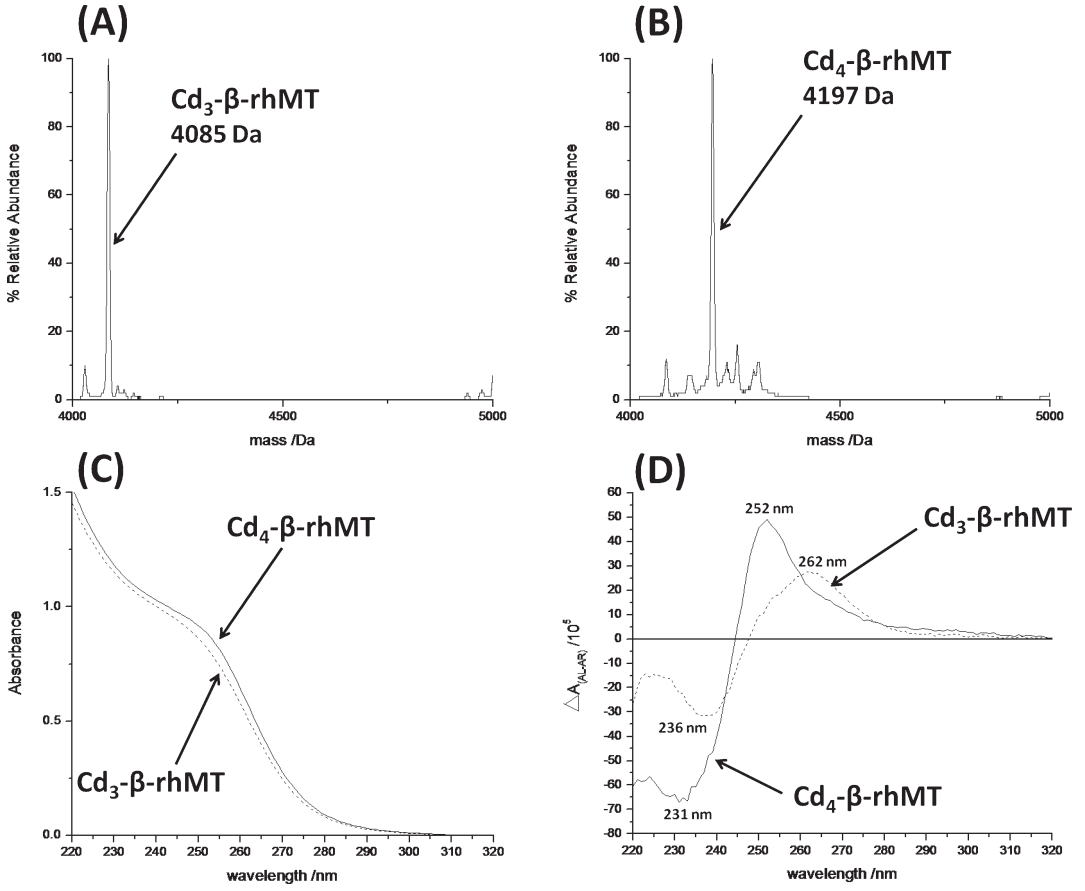

FIGURE 2: ESI-MS deconvoluted spectra, UV absorption spectra, and CD spectra of Cd_3-β-rhMT 1a and supermetalated Cd_4-β-rhMT 1a. (A) ESI-MS deconvoluted spectrum of Cd_3-β-rhMT 1a, showing the mass equal to the apoprotein with three Cd^{2+} ions. (B) ESI-MS deconvoluted spectrum of supermetalated Cd_4-β-rhMT 1a formed following the addition of 4.4 molar equiv of $CdSO_4$ to Cd_3-β-rhMT 1a, showing the additional mass from one extra Cd^{2+}. (C) UV absorption and (D) CD spectral changes observed for Cd_3-β-rhMT 1a and supermetalated Cd_4-β-rhMT 1a formed following the addition of 4.4 molar equiv of $CdSO_4$ to Cd_3-β-rhMT 1a. To ensure accurate speciation, the same samples of Cd_3-β-rhMT 1a and Cd_4-β-rhMT 1a were used in all experiments. All experiments were conducted in 5 mM ammonium formate buffer (pH 9.0) at 22 °C.

acquisition time of 1.234 s at 10 °C. The data were processed using a line broadening of 10 Hz. For Cd_4-β-rhMT 1a, a total of 84000 transients accumulated using a relaxation delay of 2 s and a 60° pulse width of 10.8 μs with an acquisition time of 0.587 s at 25 °C. The data were processed using a line broadening of 20 Hz.

Indirect 2D $^1H-^{113}Cd$ HSQC NMR spectra were recorded using a Varian indirect-detection 5.0 mm HCX probe, a ^{113}Cd spectral range from 540 to 740 ppm, a ^1H spectral range from −0.4 to 4.8 ppm, an acquisition time of 0.15 s, and a relaxation delay of 1 s. Water suppression was achieved using a selective 1 s presaturation pulse at a power of 4 dB. In the indirect ^{113}Cd dimension, the data were zero-filled to 1024 total points, and a Gaussian weighting function was applied. In the direct ^1H dimension, the data were zero-filled to 1024 points and a Gaussian weighting function was applied. For the mixture of Cd_3-β-rhMT 1a and Cd_4-β-rhMT 1a, a total of 84 transients accumulated for each of the 128 increments, a forward linear prediction of 128 points in the ^{113}Cd dimension, and the $^3J(^{113}Cd,^1H)$ value was set to 60 Hz at 30 °C. For Cd_4-β-rhMT, a total of 44 transients accumulated for each of the 256 increments, a forward linear prediction of 256 points in the ^{113}Cd dimension, and the $^3J(^{113}Cd,^1H)$ value was set to 67 Hz at 25 °C.

RESULTS

Supermetalation of β-rhMT 1a Studied by ESI-MS and CD and UV Absorption Spectroscopy. To determine the effect of the fourth metal on the overall fold of the isolated β domain, analysis with both CD and UV absorption spectroscopy, coupled with metal speciation provided by ESI-MS, was conducted. These techniques allowed us to directly correlate the number of metals bound and observed spectroscopic changes in solution. The protein used in this set of experiments was taken directly after purification and desalted into an ESI-MS compatible buffer. This was done to avoid structural changes that may occur upon acid-induced demetalation and to demonstrate that the additional low-affinity site for Cd^{2+} is not the result of high concentrations found in the NMR experiment (*32*).

A solution of Cd_3-β-rhMT 1a (Figure 2A) was initially measured. Addition of 4.4 excess molar equivalents of Cd^{2+} produced a solution with a composition of 10% Cd_3-β-rhMT and 90% Cd_4-β-rhMT (Figure 2B). The mass of apo-β-rhMT 1a is 3754 Da (spectra not shown), giving theoretical masses for Cd_3-β-rhMT 1a and Cd_4-β-rhMT 1a of 4085 and 4195 Da, respectively, which compare well with the experimental masses of 4085 and 4197 Da, respectively. Because of the weaker binding of the fourth Cd^{2+} atom to the protein, we attribute this residual 10% Cd_3-β-rhMT 1a to MS-induced dissociation of the metal. An approximate equilibrium binding constant of $(6.0 \pm 0.8) \times 10^4$ M^{-1} was determined, using the Cd_3/Cd_4 ratio based on an ESI-MS titration of apo-β-rhMT for the low-affinity site by ESI-MS, a value that is several orders of magnitude lower than previously reported binding constants for normal binding of both

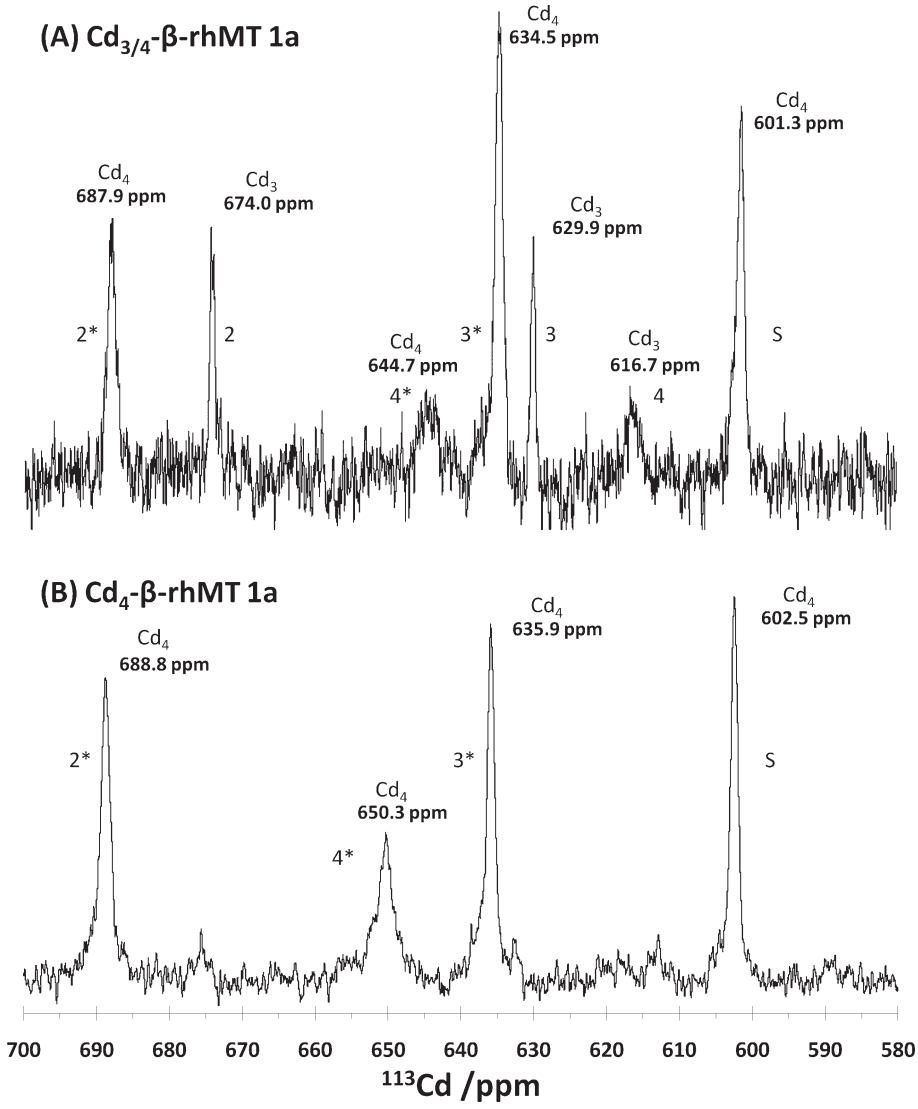

FIGURE 3: Direct 1D $^{113}Cd\{^1H\}$ NMR spectrum (133 MHz) of (A) a mixture of Cd_3-β-rhMT 1a and Cd_4-β-rhMT 1a and (B) Cd_4-β-rhMT 1a formed by addition of excess $^{113}CdCl_2$. Slight shifts in the values of Cd_4-β-rhMT 1a were observed between the mixture and the pure supermetalated sample. This shift is attributed to the addition of chloride ions from $^{113}CdCl_2$ to the solution and is most pronounced in the least intense Cd_4-β-rhMT 1a signal at 644.7 ppm, with a total downfield shift of 5.6 ppm. The mixture of Cd_3-β-rhMT and Cd_4-β-rhMT was prepared in 10 mM ammonium formate (pH 7.4) and buffer exchanged into 90% D_2O. Subsequent addition of solid $^{113}CdCl_2$ to the Cd_3-β-rhMT 1a/Cd_4-β-rhMT 1a mixture led to the formation of Cd_4-β-rhMT 1a. Spectra of the Cd_3-β-rhMT 1a/Cd_4-β-rhMT 1a mixture and Cd_4-β-rhMT 1a were recorded at 10 and 25 °C, respectively.

Cd^{2+} [$6.0 \times 10^{21}-10^{25.6}$ M^{-1} (*33*, *34*)] and Zn^{2+} [5.0×10^7 to 6.3×10^{11} M^{-1} (*35*)].

To determine the location of the fourth cadmium ion, whether it was either attached to the cluster or existed as an adduct to other opportunistic amino acids, we recorded the UV absorption and CD spectra for both Cd_3-β-rhMT 1a and Cd_4-β-rhMT 1a. While the UV spectra did not change significantly (Figure 2C), the CD spectra measured for these species (Figure 2D) showed drastic changes in the extrema. Maxima and minima at 262 and 236 nm, respectively, were observed for Cd_3-β-rhMT 1a, while Cd_4-β-rhMT 1a exhibited maxima and minima of 252 and 231 nm, respectively. For Cd_3-β-rhMT 1a, the maximum at 262 nm was broad, suggesting that the traditional structure is flexible and exists as a mixture of conformations.

Upon addition of excess Cd^{2+} to solution, the maximum blue-shifted to 252 nm and the intensity increased by 60%. The increase in intensity may be attributed to a decrease in the conformational flexibility of the protein, while the blue shift can be associated with a breaking of the exciton coupling between the three Cd^{2+} ions of the system as observed when Cd_5-α-rhMT 1a is formed (*12*). The breaking of exciton coupling strongly suggests that the fourth Cd^{2+} atom is involved in the metal−thiolate cluster. A previous analysis of the β domain using mouse MT-1 demonstrated CD spectral changes between 3 and 12 equiv of Cd^{2+} (*36*), which the author argued was the result of a Cd_9-β-rhMT 1, but which we postulate to be supermetalated Cd_4-β-rhMT 1.

1D ^{113}Cd NMR Spectroscopy of Cd_3-β-rhMT 1a and Cd_4-β-rhMT 1a. Direct 1D $^{113}Cd\{^1H\}$ NMR spectroscopy was used for a mixture of Cd_3-β-rhMT 1a and Cd_4-β-rhMT 1a, a result of a slight excess of Cd^{2+} to increase resistance to oxidation, and a pure sample of Cd_4-β-rhMT 1a to determine the relative speciation of the individual metal binding sites as well as the type of coordinating ligands through chemical shift data. Samples were isotopically enriched with $^{113}CdCl_2$ in 10 mM ammonium formate (pH 7.4), following demetalation with formic acid, to enhance the NMR signal. Signals observed for Cd_3-β-rhMT 1a and Cd_4-β-rhMT 1a (Figure 3A) include those at 687.9, 674.0, 644.7, 634.5, 629.9, 616.7, and 601.3 ppm, while the

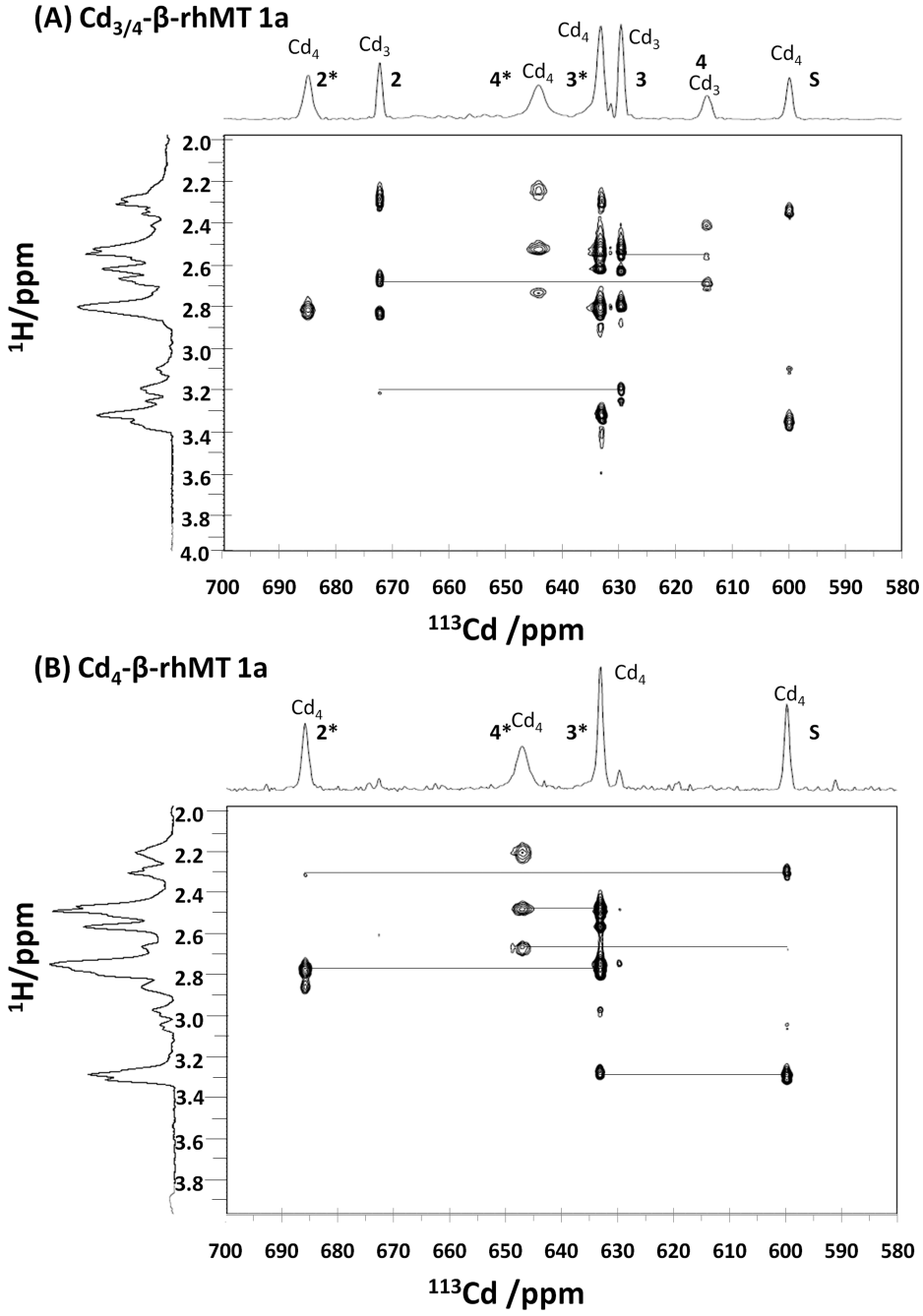

FIGURE 4: Indirect 2D $^{1}H\{^{113}Cd\}$ HSQC NMR spectra of (A) a mixture of Cd_3-β-rhMT 1a and Cd_4-β-rhMT 1a and (B) Cd_4-β-rhMT 1a formed by addition of excess $^{113}CdCl_2$. The spectra were recorded in the ^{1}H chemical shift range of -0.4 to 4.8 ppm and the ^{113}Cd chemical shift range of 540−740 ppm (^{3}J = 60 and 67 Hz) for Cd_3-β-rhMT and Cd_4-β-rhMT, respectively. Spectrum A was recorded at 30 °C, while spectrum B was recorded at 25 °C. Both spectra were acquired using an inverse single-axis z-gradient HCX probe with X tuned to ^{113}Cd. These spectra were used to aid in correlating Cd_3-β-rhMT peaks with Cd_4-β-rhMT peaks.

observed signals for pure Cd_4-β-rhMT 1a (Figure 3B) are at 688.8, 650.3, 635.9, and 602.5 ppm. The chemical shift range of all the peaks is between 600 and 700 ppm, which overlaps significantly with the region expected for tetrahedral cadmium−thiolate clusters (*37*), traditional of metallothioneins, as well as both trigonal and tetrahedral cadmium−thiolate clusters in which a single sulfur has been replaced with water (*38*). By comparison of the signals from both sets of data, the peaks for Cd_3-β-rhMT 1a can be identified as 674.0, 629.9, and 616.7 ppm. Previous NMR work on human liver MT-1 has shown chemical shifts of 670.5, 652.0, and 645.8 ppm for the β domain (*24*); the differences in the chemical shifts are most likely due to the lack of the α domain as well as differences in sample conditions.

Direct detection of ^{113}Cd in the binding site allows one to infer the fluxionality of the individual metal ions. Analysis of the spectrum in Figure 3A shows that peaks attributed to Cd_3-β-rhMT 1a species, with the exception of 674.0 ppm, are significantly less intense than those we attribute to Cd_4-β-rhMT 1a. Previous NMR studies involving both domains have suggested that the α domain is less fluxional than the β domain, leading to sharper peaks of greater intensity (*24*). Upon addition of excess $^{113}Cd^{2+}$ to solution, the observed chemical shifts of Cd_3-β-rhMT 1a almost completely disappear with an increase in intensity of the peaks assigned to Cd_4-β-rhMT 1a, suggesting an overall reduction in the fluxionality of Cd_4-β-rhMT 1a compared to Cd_3-β-rhMT 1a. There is a slight chemical shift in each of the four

peaks, with the most significant shift being a total of 5.6 ppm involving the movement from 644.7 to 650.3 ppm, attributed to the increase in the number of chloride ions from $^{113}CdCl_2$ (*39*). This peak is also noticeably broader and less intense than the other three, which are of comparable size, suggesting that this binding site is more solvent-exposed and fluxional. The increase in fluxionality and the level of solvent exposure of just this site would make this Cd^{2+} site the most likely candidate for the metal-exchange intermediate, allowing both the solvent and acceptor and donor proteins access to the metal. The sharpness of the spectral lines further supports the interpretation of CD spectroscopic data that the maximum blue shift between Cd_3-β-rhMT 1a and Cd_4-β-rhMT 1a, with an increase in intensity of 60%, is the result of a reduction in the fluxionality of the domain overall.

2D $^1H\{^{113}Cd\}$ HSQC NMR Spectroscopy of both Cd_3-β-rhMT 1a and Cd_4-β-rhMT 1a. Indirect $^1H\{^{113}Cd\}$ HSQC NMR spectroscopy was used for both the Cd_3-β-rhMT 1a/Cd_4-β-rhMT 1a mixture and Cd_4-β-rhMT 1a (Figure 4). Analysis of the β protons of the cysteine residues allowed determination of peak relatedness as well as a tentative assignment of the metal−thiolate connectivity. Peaks were interpreted as related on the basis of the similarity in both the ^1H and ^{113}Cd chemical shifts. Changes in the chemical shifts of the β protons were observed for all metal sites existing in both Cd_3-β-rhMT and Cd_4-β-rhMT, and it is likely these are the result of the structural changes necessary for the accommodation of a fourth cadmium atom in the β metal−thiolate cluster. In Figure 4, peak 2* possessed intense signals that could be observed at both 2.3 and 2.8 ppm in the ^1H dimension; both signals overlapped well with peaks assigned to peak 2. The similarity of both the ^1H profile and the ^{113}Cd chemical shift range suggests that they are related. Peaks 3 and 3*, from Cd_3-β-rhMT 1a and Cd_4-β-rhMT 1a, respectively, were interpreted as related with both similar peak shape and profile from 2.4 to 3.5 ppm. A slight downfield shift can be seen in signals, in the 3.2−3.4 ppm ^1H range, from the β protons associated with peak 3*, Cd_4-β-rhMT 1a, relative to peak 3, Cd_3-β-rhMT 1a. Assignment of the cadmium center associated with peaks 4 and 4* was based on the significant similarity in the β proton region. Additionally, these peaks are equally broad and have comparable intensities in the 1D $^{113}Cd\{^1H\}$ NMR spectrum (Figure 3A). The new signal, S, is attributed to the supermetalated site and is significantly upfield from all other cadmium peaks. At 602.5 ppm, this peak may represent a tetrahedral geometry coordinating either four thiolates or three thiolates and a single water molecule or chloride ion.

Assignment of the HSQC spectrum for Cd_3-β-rhMT 1a shows three bridging cysteine residues (Figure 4A), as one would expect from the connectivity (Figure 1). Upon addition of excess cadmium, two additional bridging interactions are observed. Interestingly, the new metal appears to coordinate with all other metal centers at the expense of bridging interactions within the original cluster. It is this loss of original bridging interactions that may explain the loss of exciton coupling in CD spectroscopy without any significant change in the ligand-to-metal charge transfer band observed in UV spectroscopy (Figure 2).

DISCUSSION

It has been proposed over the past 50 years that various different metallothioneins perform many critical functions related to metal homeostasis, metal exchange, and recently cellular redox status. In this study, analysis of the spectroscopic data from metalation of the β domain of human metallothionein 1a has shown that a supermetalated form of the domain exists (the extra metal ion is located in the metal thiolate cluster), and we propose that this supermetalated form, with a distorted cluster, may be a model of the metal-exchange intermediate.

Prior to this report, it was unclear whether an additional metal was bound to the protein metal−thiolate core or if the protein was somehow bound to other ligands. However, the coupling of both spectroscopic and spectrometric analyses demonstrates that addition of an excess of Cd^{2+} to the fully metalated peptide causes significant rearrangement of the cluster. This rearrangement leads to a breaking of the symmetry of the cluster, through a loss of exciton coupling, but with little change in the ligand-to-metal charge transfer profile (Figure 2).

Both direct and indirect ^{113}Cd NMR spectroscopy provided tentative connectivities. An increase in the number of bridging interactions, from 3 to 5, was observed. The newly coordinated metal bridges with all three of the original metals at the cost of cluster symmetry, explaining the change in the CD spectrum. We propose an increase in the number of bridging interactions, as the protein cluster expands, may be critical for the functions of metal ion homeostasis and toxic metal detoxification because formation of these new bonds may be the first step in metal insertion, followed by expulsion of one of the originally coordinated metals.

This insertion−expulsion mechanism would allow Cd^{2+}, which binds several orders of magnitude more tightly than Zn^{2+}, to exchange with Zn^{2+}-bound metallothionein simultaneously acting to sequester toxic Cd^{2+} and releasing Zn^{2+}. The net effect would be upregulation of metallothionein, allowing an organism to effectively combat toxic metal exposure. A regulator of metallothionein transcription, metal-responsive-element-binding transcription factor-1 (MTF-1), has been shown to upregulate metallothionein upon binding to Zn^{2+} (*40*). MTF-1 has been implicated in cellular responses, including toxic metal detoxification and oxidative stress, both of which are implicated functions of metallothionein. The metal binding site of this transcription factor includes six Cys_2His_2 zinc fingers, making it exceptionally sensitive to an organism's zinc load. We describe this property of supermetalation in the context of metal transfer whereby metals bound to MT are transferred to metal-free apoproteins, so that these structures represent the intermediates of these transfer reactions. Of course, as intermediates they have virtually zero population. However, in the case of Cd-containing MT-1, we find the supermetalated form to be stable, in essence frozen between the two states. A second scenario is that of the influx of a metal with a greater binding affinity than the resident metal. In the case of Cd^{2+} displacing a resident Zn^{2+}, these structures may represent the intermediate as the Cd^{2+} enters the clusters prior to the Zn^{2+} being displaced. This would be a critically important transient species in the regulation of transcription of the protein. An incoming metal, such as cadmium(II) or copper(I), could coordinate in a supermetalated position, allowing both sequestration of the metal and release of a zinc ion. This zinc ion would consequently lead to the upregulation of MT, through MTF-1, allowing an organism to effectively bind a greater number of incoming metals. For a toxic metal such as Cd^{2+}, the mechanism allows for a fast response to the influx of a potentially damaging metal. Indeed, we believe that these supermetalated structures may also be involved in the redistribution of Zn^{2+} between domains, but we have no experimental evidence to support this model. Overall, through supermetalation, the organism may be able to control the cellular levels of free metals.

Supermetalation has now been reported in the α domain, Cd_5-α-rhMT 1a, β domain, Cd_4-β-rhMT 1a, and full protein, Cd_8-βα-rhMT 1a, of human metallothionein 1a (*7*, *28*). In the case of the α domain of human MT-1, analysis of ^{113}Cd NMR spectra provided data suggesting that the supermetalated form, Cd_5-α-rhMT 1a, included two bridging interactions through a crevice located on the α domain. ESI-MS titrations have also provided evidence that a supermetalated Cd_8-βα-rhMT 1a may exist in a dynamic equilibrium with Cd_7-βα-rhMT. Chan et al. attributed supermetalation of the full protein to supermetalation of the α domain, with the β domain remaining intact (*28*). Currently, no competition experiments between the two isolated domains have been performed that would allow the determination of the relative affinity of Cd^{2+} in forming supermetalated species for either of the two domains; however, the NMR chemical shifts would suggest that supermetalation first occurs in the β domain. By comparison, supermetalation of the α domain produces a peak at 224 ppm, while supermetalation of the β domain produces a peak at 602 ppm. The dramatic difference in peak locations suggests that there are more cysteine residues coordinating the Cd^{2+} involved in the supermetalated β domain than there are in the α domain. These cysteine residues would act to stabilize the supermetalated structure, leading to an increase in the affinity of the β domain for Cd^{2+} and Zn^{2+} metal ions.

Supermetalation of the brain specific MT-3 to produce Cd_8-βα-hMT 3 has also been observed (*13*). Unlike supermetalation of MT-1, Meloni et al. have suggested that both domains bridge together to accommodate the eighth cadmium atom. Interestingly, comparison of metallothionein isoforms MT-2 and MT-3 demonstrated that while MT-3 was capable of accepting an additional metal ion, MT-2 was not. However, both MT-1 and MT-2 are more closely related than MT-3, the former having diverged before distinction of the mammalian orders and the latter, more structurally distinct, having evolved much earlier (*41*). Surprisingly, Romero-Isart et al. demonstrated the ability to confer neuroinhibitory MT-3 activity onto MT-1 (*21*), through a series of mutations of the β domain. We postulate that supermetalation, a property observed only in distantly related MT-1 and MT-3, may be a factor that leads to the differentiation of each isoform into specific functions in cellular chemistry.

One important aspect that must be examined further is the exact location of the low-affinity binding site(s) on the Cd_8-βα-hMT (1 or 3) protein. Figure 5 compares the NMR spectral data for human Cd_7-βα-MT 1, 2, and 3, the two isolated fragments of Cd_3-β-rhMT 1a and Cd_4-α-rhMT 1a, and the supermetalated species, Cd_4-β-rhMT 1a and Cd_5-α-rhMT 1a. The value of this figure is to show how the extra metal for the β domain described here exhibits a typical ^{113}Cd NMR spectral signature that falls within the range of MT data. Indeed, it is possible that the Cd_7-βα-hMT 1 spectrum may contain a small fraction of Cd_4-β-hMT as indicated by an overlap of the NMR signals of Cd_4-β-rhMT 1a with those of Cd_7-βα-hMT 1. On the other hand, the fifth Cd^{2+} in Cd_5-α-rhMT 1a results in a resonance in the region well away from the tetrahedral thiolates. Two possibilities exist for the location of the low-affinity sites on Cd_8-βα-hMT: (1) each domain is independently capable of binding an additional metal ion, as supported by supermetalation of the isolated β and α domains of MT-1, or (2) the two domains work in concert to bind this additional metal, as supported by the decrease in the Stokes radius of MT-3 upon supermetalation, which is consistent with the close approach of both clusters. It is probable that supermetalation of metallothionein is isoform specific, related to cellular function, and mechanisms of metalation must be determined on a case-by-case basis. Answers to these questions in the future will have consequences for metal ion homeostasis, as well as toxic metal detoxification, and could possibly lead to an assignment of a specific function for each of the metallothionein isoforms.

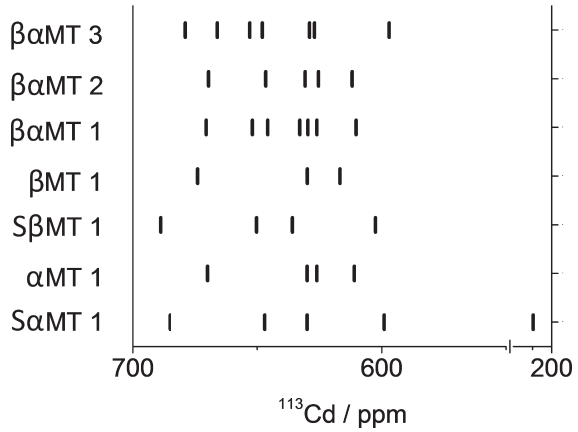

FIGURE 5: Comparison of the ^{113}Cd NMR resonances for human MTs: Cd_7-βα-hMT 3 (*15*), Cd_7-βα-hMT 2 (*24*), Cd_7-βα-hMT 1 (*24*), Cd_3-β-rhMT 1a (this work), supermetalated Cd_4-β-rhMT 1a (this work), Cd_4-α-rhMT 1a (*12*), and supermetalated Cd_5-α-rhMT 1a (*12*). We note that in this diagram, for the spectrum of Cd_7-βα-MT 2, the resolution precludes separation of overlapping resonances 1 and 2 (near 670 ppm) and 3 and 4 (near 645 ppm), so that in total there are seven resonances.

ACKNOWLEDGMENT

We thank Prof. R. J. Puddephatt for use of the ESI-MS instrument funded by the Canada Research Chair program, Doug Hairsine for advice and discussion on the operation of the ESI-MS instrument, and John Vanstone for NMR probe refurbishment.

REFERENCES

1. Margoshes, M., and Vallee, B. L. (1957) A Cadmium Protein From Equine Kidney Cortex. *J. Am. Chem. Soc. 79*, 4813–4814.
2. Kang, Y. J. (2006) Metallothionein Redox Cycle and Function. *Exp. Biol. Med. 231*, 1459–1467.
3. Maret, W. (2008) A role for metallothionein in the pathogenesis of diabetes and its cardiovascular complications. *Mol. Gen. Metab. 94*, 1–3.
4. Good, M., Hollenstein, R., Sadler, P. J., and Vasak, M. (1988) ^{113}Cd NMR Studies on Metal-Thiolate Cluster Formation in Rabbit Cd(II)-Metallothionein: Evidence for a pH Dependence. *Biochemistry 27*, 7163–7166.
5. Gehrig, P. M., You, C., Dallinger, R., Gruber, C., Brouwer, M., Kagi, J. H. R., and Hunziker, P. E. (2000) Electrospray ionization mass spectrometry of zinc, cadmium, and copper metallothioneins: Evidence for metal-binding cooperativity. *Protein Sci. 9*, 395–402.
6. Palumaa, P., Eriste, E., Njunkova, O., Pokras, L., Jornvall, H., and Sillard, R. (2002) Brain-Specific Metallothionein-3 Has Higher Metal-Binding Capacity than Ubiquitous Metallothioneins and Binds Metals Noncooperatively. *Biochemistry 41*, 6158–6163.
7. Duncan, K. E. R., and Stillman, M. J. (2007) Evidence for non-cooperative metal binding to the α domain of human metallothionein. *FEBS J. 274*, 2253–2261.
8. Sutherland, D. E. K., and Stillman, M. J. (2008) Noncooperative cadmium(II) binding to human metallothionein 1a. *Biochem. Biophys. Res. Commun. 372*, 840–844.
9. Ngu, T. T., Easton, A., and Stillman, M. J. (2008) Kinetic Analysis of Arsenic-Metalation of Human Metallothionein: Significance of the Two-Domain Structure. *J. Am. Chem. Soc. 130*, 17016–17028.
10. Ngu, T. T., Lee, J. A., Rushton, M. K., and Stillman, M. J. (2009) Arsenic Metalation of Seaweed *Fucus vesiculosus* Metallothionein: The Importance of the Interdomain Linker in Metallothionein. *Biochemistry 48*, 8806–8816.

11. Nielson, K. B., Atkin, C. L., and Winge, D. R. (1985) Distinct Metal-binding Configurations in Metallothionein. *J. Biol. Chem. 260*, 5342–5350.
12. Duncan, K. E. R., Kirby, C. W., and Stillman, M. J. (2008) Metal exchange in metallothioneins: A novel structurally significant Cd_5 species in the α domain of human metallothionein 1a. *FEBS J. 275*, 2227–2239.
13. Meloni, G., Polanski, T., Braun, O., and Vasak, M. (2009) Effects of Zn^{2+}, Ca^{2+}, and Mg^{2+} on the Structure of Zn_7Metallothionein-3: Evidence for an Additional Zinc Binding Site. *Biochemistry 48*, 5700–5707.
14. Wang, H., Li, H., Cai, B., Huang, Z.-X., and Sun, H. (2008) The effect of nitric oxide on metal release from metallothionein-3: Gradual unfolding of the protein. *J. Biol. Inorg. Chem. 13*, 411–419.
15. Wang, H., Zhang, Q., Cai, B., Li, H., Sze, K.-H., Huang, Z.-X., Wu, H.-M., and Sun, H. (2006) Solution structure and dynamics of human metallothionein-3 (MT-3). *FEBS Lett. 580*, 795–800.
16. Braun, W., Vasak, M., Robbins, A. H., Stout, C. D., Wagner, G., Kagi, J. H. R., and Wuthrich, K. (1992) Comparison of the NMR solution structure and the X-ray crystal structure of rat metallothionein-2. *Proc. Natl. Acad. Sci. U.S.A. 89*, 10124–10128.
17. Morris, C. A., Nicolaus, B., Sampson, V., Harwood, J. L., and Kille, P. (1999) Identification and characterization of a recombinant metallothionein protein from a marine alga, *Fucus vesiculosus*. *Biochem. J. 338*, 553–560.
18. Leszczyszyn, O. I., Evans, C. D., Keiper, S. E., Warren, G. Z. L., and Blindauer, C. A. (2007) Differential reactivity of individual zinc ions in clusters from bacterial metallothioneins. *Inorg. Chim. Acta 360*, 3–13.
19. Peroza, E. A., Schmucki, R., Guntert, P., Freisinger, E., and Zerbe, O. (2009) The β_E-Domain of Wheat E_c-1 Metallothionein: A Metal-Binding Domain with a Distinctive Structure. *J. Mol. Biol. 387*, 207–218.
20. Uchida, Y., Takio, K., Titani, K., Ihara, Y., and Tomonaga, M. (1991) The growth inhibitory factor that is deficient in the Alzheimer's disease brain is a 68 amino acid metallothionein-like protein. *Neuron 7*, 337–347.
21. Romero-Isart, N., Jensen, L. T., Zerbe, O., Winge, D. R., and Vasak, M. (2002) Engineering of Metallothionein-3 Neuroinhibitory Activity into the Inactive Isoform Metallothionein-1. *J. Biol. Chem. 277*, 37023–37028.
22. Zheng, Q., Yang, W.-M., Yu, W.-H., Cai, B., Teng, X.-C., Xie, Y., Sun, H.-Z., Zhang, M.-J., and Huang, Z.-X. (2003) The effect of the EAAEAE insert on the property of human metallothionein-3. *Protein Eng. 16*, 865–870.
23. Sewell, A. K., Jensen, L. T., Erickson, J. C., Palmiter, R. D., and Winge, D. R. (1995) Bioactivity of Metallothionein-3 Correlates with Its Novel β Domain Sequence Rather Than Metal Binding Properties. *Biochemistry 34*, 4740–4747.
24. Boulanger, Y., and Armitage, I. M. (1982) ^{113}Cd NMR Study of the Metal Cluster Structure of Human Liver Metallothionein. *J. Inorg. Biochem. 17*, 147–153.
25. Boulanger, Y., Armitage, I. M., Miklossy, K.-A., and Winge, D. R. (1982) ^{113}Cd NMR Study of a Metallothionein Fragment. *J. Biol. Chem. 257*, 13717–13719.
26. Calderone, V., Dolderer, B., Hartmann, H.-J., Echner, H., Luchinat, C., Bianco, C. D., Mangani, S., and Weser, U. (2005) The crystal structure of yeast copper thionein: The solution of a long-lasting enigma. *Proc. Natl. Acad. Sci. U.S.A. 102*, 51–56.
27. Messerle, B. A., Schaffer, A., Vasak, M., Kagi, J. H. R., and Wuthrich, K. (1990) Three-dimensional Structure of Human [$^{113}Cd_7$]Metallothionein-2 in Solution Determined by Nuclear Magnetic Resonance Spectroscopy. *J. Mol. Biol. 214*, 765–779.
28. Chan, J., Huang, Z., Watt, I., Kille, P., and Stillman, M. J. (2007) Characterization of the conformational changes in recombinant human metallothioneins using ESI-MS and molecular modeling. *Can. J. Chem. 85*, 898–912.
29. Feng, W., Cai, J., Pierce, W. M., Franklin, R. B., Maret, W., Benz, F. W., and Kang, Y. J. (2005) Metallothionein transfers zinc to mitochondrial aconitase through a direct interaction in mouse hearts. *Biochem. Biophys. Res. Commun. 332*, 853–858.
30. Mason, A. Z., Perico, N., Moeller, R., Thrippleton, K., Potter, T., and Lloyd, D. (2004) Metal donation and apo-metalloenzyme activation by stable isotopically labeled metallothionein. *Mar. Environ. Res. 58*, 371–375.
31. Maret, W., Larsen, K. S., and Vallee, B. L. (1997) Coordination dynamics of biological zinc "clusters" in metallothioneins and in the DNA-binding domain of the transcription factor Gal4. *Proc. Natl. Acad. Sci. U.S.A. 94*, 2233–2237.
32. Ejnik, J. W., Munoz, A., DeRose, E., Shaw, F. C., III, and Petering, D. H. (2003) Structural Consequences of Metallothionein Dimerization: Solution Structure of the Isolated Cd_4-α-Domain and Comparison with the Holoprotein Dimer. *Biochemistry 42*, 8403–8410.
33. Zhang, B. L., Sun, W. Y., and Tang, W. X. (1997) Determination of the Association Constant of Platinum(II) to Metallothionein. *J. Inorg. Biochem. 65*, 295–298.
34. Kagi, J. H. R., and Vallee, B. L. (1961) Metallothionein: A Cadmium- and Zinc-containing Protein from Equine Renal Cortex. *J. Biol. Chem. 236*, 2435–2442.
35. Krezel, A., and Maret, W. (2007) Dual Nanomolar and Picomolar Zn(II) Binding Properties of Metallothionein. *J. Am. Chem. Soc. 129*, 10911–10921.
36. Capdevila, M., Cols, N., Romero-Isart, N., Gonzalez-Duarte, R., Atrian, S., and Gonzalez-Duarte, P. (1997) Recombinant synthesis of mouse Zn_3-β and Zn_4-α metallothionein 1 domains and characterization of their cadmium(II) binding capacity. *Cell. Mol. Life Sci. 53*, 681–688.
37. Ellis, P. D. (1983) Cadmium-113 Magnetic Resonance Spectroscopy. *Science 221*, 1141–1146.
38. Iranzo, O., Jakusch, T., Lee, K.-H., Hemmingsen, L., and Pecoraro, V. L. (2009) The Correlation of ^{113}Cd NMR and ^{111m}Cd PAC Spectroscopies Provides a Powerful Approach for the Characterization of the Structure of Cd^{II}-Substituted Zn^{II} Proteins. *Chem.—Eur. J. 15*, 3761–3772.
39. Villarreal, L., Tio, L., Atrian, S., and Capdevila, M. (2005) Influence of chloride ligands on the structure of Zn- and Cd- metallothionein species. *Arch. Biochem. Biophys. 435*, 331–335.
40. Laity, J. H., and Andrews, G. K. (2007) Understanding the mechanisms of zinc-sensing by metal-response element binding transcription factor-1 (MTF-1). *Arch. Biochem. Biophys. 463*, 201–210.
41. Kagi, J. H. R. (1993) Evolution, Structure and Chemical Activity of Class I Metallothioneins: An Overview. In Metallothionein III: Biological Roles and Medical Implications (Suzuki, K. T., Imura, N., and Kimura, M., Eds.) Birkhäuser-Verlag, Berlin.